

Unsupervised Deep Generative Adversarial Hashing Network

Kamran Ghasedi Dizaji¹, Feng Zheng¹, Najmeh Sadoughi¹, Yanhua Yang², Cheng Deng², Heng Huang¹

kag221@pitt.edu, feng.zheng@pitt.edu, najme.sadoughi@gmail.com, yanhyang@xidian.edu.cn, chdeng.xd@gmail.com, heng.huang@pitt.edu

¹Electrical and Computer Engineering Department, University of Pittsburgh, PA, USA

²Xidian University, Xi'an, Shanxi, China

Challenges

- Unsupervised hashing methods either utilize **shallow** models with hand-crafted features as inputs, or employ **deep** architectures for obtaining both discriminative features and binary hash codes.
- The shallow hash functions suffer from **hand-crafted features** and **dimension reductions techniques**, and may not capture the **non-linear** similarities between real-world images due to their low capacity.
- The unsupervised deep hash functions have not shown satisfactory **improvements** against their shallow alternatives due to **overfitting** problem in lack of any supervisory signals.

Contributions

- We propose a novel framework for unsupervised hashing model by coupling a **deep hash function** and a **generative adversarial network**.
- We introducing a new hashing objective resulting in minimum entropy, uniform frequency, consistent, and independent hash bits for real images, regularized by the **adversarial and collaborative loss functions** on synthesized images.
- Achieving state-of-the-art results compared to alternative models on **information retrieval** and **clustering** tasks.

HashGAN Objective Function

- General loss

$$\mathcal{L}_{total} = \mathcal{L}_{adv} + \mathcal{L}_{hash} + \mathcal{L}_{col}$$

- Adversarial loss

$$\max_{\mathcal{D}} \mathbb{E}_{\mathbf{x} \sim P(\mathbf{x})} [\log(\mathcal{D}(\mathbf{x}))] + \mathbb{E}_{\mathbf{z} \sim P(\mathbf{z})} [\log(1 - \mathcal{D}(\mathcal{G}(\mathbf{z})))]$$

- Hashing loss

$$\min_{\mathcal{E}} - \underbrace{\sum_{i=1}^N \sum_{k=1}^K t_{ik} \log t_{ik} + (1 - t_{ik}) \log(1 - t_{ik})}_{\text{minimum entropy bits}} + \underbrace{\sum_{i=1}^N \sum_{k=1}^K \|t_{ik} - \tilde{t}_{ik}\|_2^2}_{\text{consistent bits}} + \underbrace{\sum_{k=1}^K f_k \log f_k + (1 - f_k) \log(1 - f_k)}_{\text{uniform frequency bits}} + \underbrace{\|\mathbf{W}_{\mathcal{E}}^L \mathbf{W}_{\mathcal{E}}^L - \mathbf{I}\|_2^2}_{\text{independent bits}}$$

- Collaborative loss

$$\min_{\mathcal{E}} \mathbb{E}_{\mathbf{z} \sim P(\mathbf{z})} [\|\mathcal{E}(\mathcal{G}(\mathbf{z})) - \mathbf{b}'\|_2^2]$$

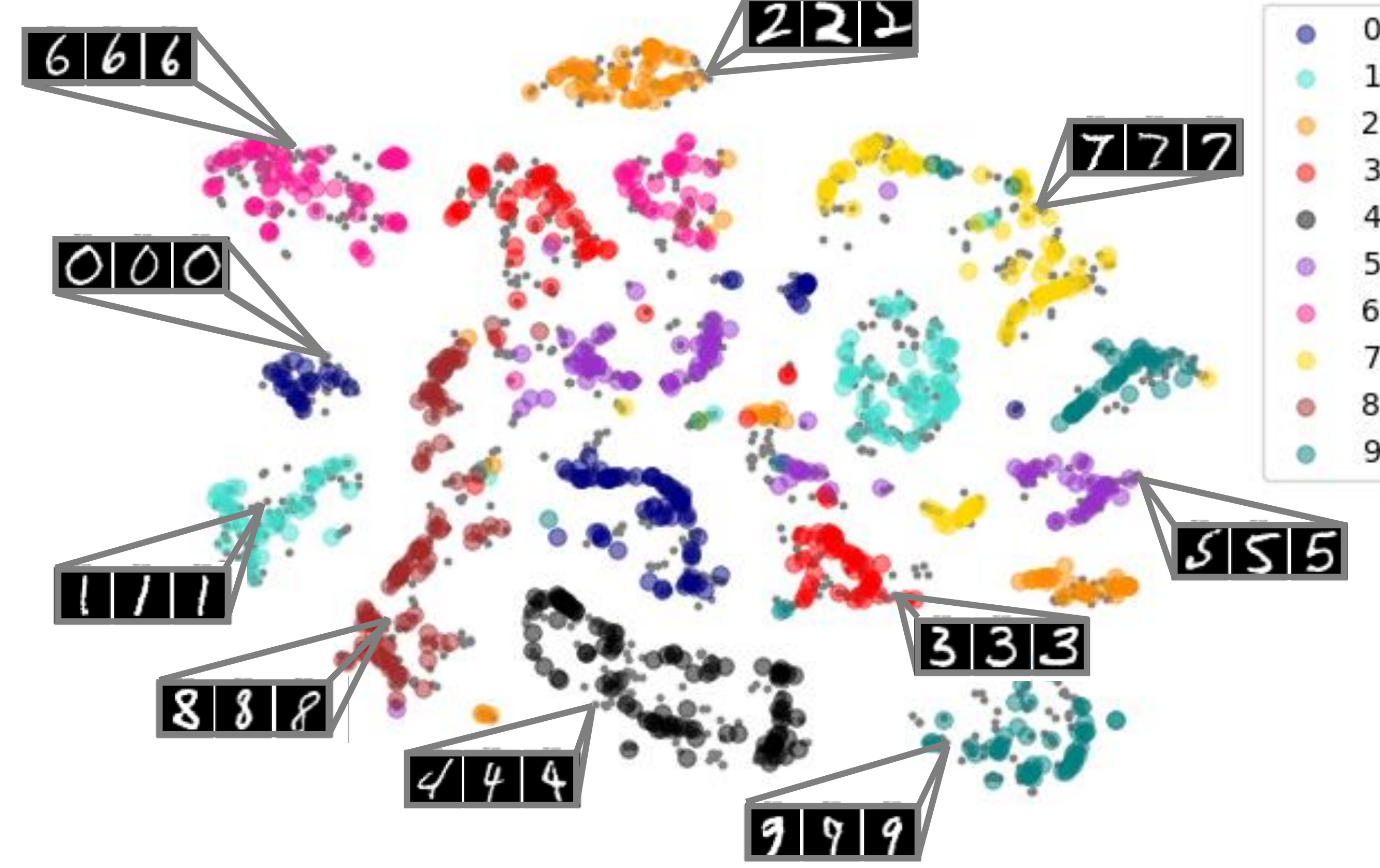


Figure 1: Visualization of HashGAN discriminative representations for a query set on MNIST using TSNE projection. The real and synthesized data are indicated by colored and gray circles respectively. Some of the synthesized images are randomly shown from different parts of space.

	Dataset	CIFAR-10						MNIST						Super
		mAP (%)			mAP@1000 (%)			mAP (%)			mAP@1000 (%)			
	Model	16	32	64	16	32	64	16	32	64	16	32	64	
Shallow	KMH	13.59	13.93	14.46	24.08*	23.56*	25.19*	32.12	33.29	35.78	59.12*	70.32*	67.62*	✗
	SphH	13.98	14.58	15.38	24.52*	24.16*	26.09*	25.81	30.77	34.75	52.97*	65.45*	65.45*	✗
	SpeH	12.55	12.42	12.56	22.10*	21.79*	21.97*	26.64	25.72	24.10	59.72*	64.37*	67.60*	✗
	PCAH	12.91	12.60	12.10	21.52*	21.62*	20.54*	27.33	24.85	21.47	60.98*	64.47*	63.31*	✗
	LSH	12.55	13.76	15.07	12.63*	16.31*	18.00*	20.88	25.83	31.71	42.10*	50.45*	66.23*	✗
	ITQ	15.67	16.20	16.64	26.71*	27.41*	28.93*	41.18	43.82	45.37	70.06*	76.86*	80.23*	✗
Deep	DH	16.17	16.62	16.96	-	-	-	43.14	44.97	46.74	-	-	-	✗
	DAR	16.82	17.01	17.21	-	-	-	-	-	-	-	-	-	✗
	DeepBit	-	-	-	19.43	24.86	27.73	-	-	-	28.18	32.02	44.53	✓
	UTH	-	-	-	28.66	30.66	32.41	-	-	-	43.15	46.58	49.88	✓
	HashGAN	29.94	31.47	32.53	44.65	46.34	48.12	91.13	92.70	93.93	94.31	95.48	96.37	✗

Table 1: Image retrieval results (mAP and mAP@1000) of unsupervised hash functions on CIFAR-10 and MNIST datasets, when the number of hash bits are 16, 32 and 64. The usage of supervised pretraining is shown for each model using the tick sign.

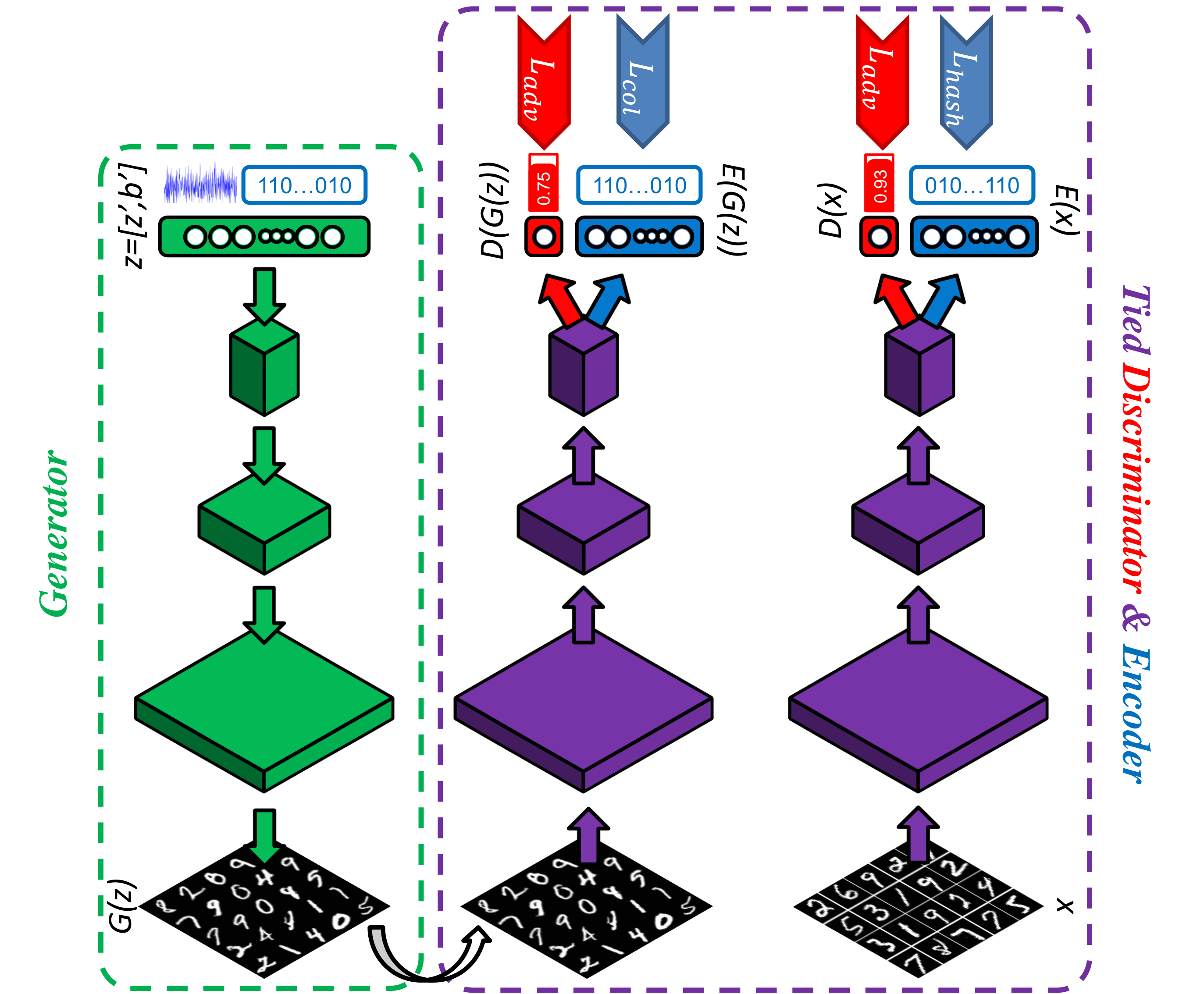


Figure 2: HashGAN architecture, including a generator (green), a discriminator (red) and an encoder (blue), where the last two share their parameters in several layers (red ⊕ blue = purple). The arrows on top represent the loss functions.

	Dataset	MNIST		USPS		FRGC		STL-10	
		NMI	ACC	NMI	ACC	NMI	ACC	NMI	ACC
Shallow	K-means	0.500	0.534	0.450	0.460	0.287	0.243	0.209*	0.284
	N-Cuts	0.411	0.327	0.675	0.314	0.285	0.235	-	-
	SC-LS	0.706	0.714	0.681	0.659	0.550	0.407	-	-
	AC-PIC	0.017	0.115	0.840	0.855	0.415	0.320	-	-
	SEC	0.779	0.804	0.511	0.544	-	-	0.245*	0.307
	LDMGI	0.802	0.842	0.563	0.580	-	-	0.260*	0.331
Deep	NMF-D	0.152	0.175	0.287	0.382	0.259	0.274	-	-
	DEC	0.816	0.844	0.586	0.619	0.505	0.378	0.284*	0.359
	JULE-RC	0.913	0.964	0.913	0.950	0.574	0.461	-	-
	DEPICT	0.917	0.965	0.927	0.964	0.610	0.470	0.303*	0.371*
	HashGAN	0.913	0.965	0.920	0.958	0.602	0.465	0.316	0.394

Table 2: Clustering performance of HashGAN and several other algorithms on four image datasets based on accuracy (ACC) and normalized mutual information (NMI).

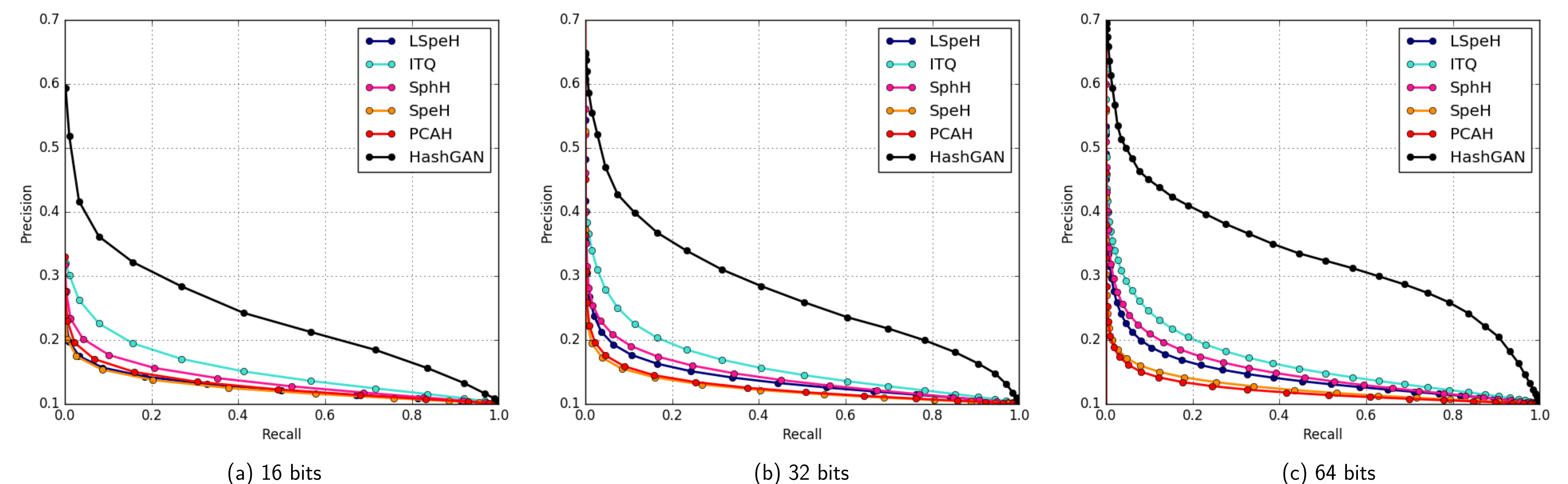


Figure 3: Precision-Recall curves on CIFAR-10 database for HashGAN and five baselines with 16, 32, and 64 hash bits.